

Electronic Supplementary Information (ESI)

Monolayer Graphene-supported Free-standing PS-*b*-PMMA Thin Film with Perpendicularly Orientated Microdomains

Mei-Ling Wu,^{ab} Jing Li,^{ab} Li-Jun Wan,^a and Dong Wang^{*a}

^a Kay Laboratory of Molecular Nanostructure and Nanotechnology and Beijing National Laboratory for Molecular Sciences, Institute of Chemistry, Chinese Academy of Sciences (CAS), Beijing 100190, P. R. China.

^b University of CAS, Beijing 100049, P. R. China

* To whom correspondence should be addressed. E-mail: wangd@iccas.ac.cn

Experimental Section

Growth and Modification of Graphene: Monolayer graphene was synthesized on copper foil by the chemical vapor deposition method. A 25 μm thick copper foil (99.8%, Alfa Aesar) was put in a corundum tube and annealed at 1000 $^{\circ}\text{C}$ for 30 min in a H_2/Ar flow. The copper foil was then further treated in CH_4/H_2 gas at 1050 $^{\circ}\text{C}$ for 60 min to yield monolayer graphene. The freshly grown graphene on copper foil was treated on an UV/Ozone (UVO) cleaner (SAMCO Inc. Japan) for different time in O_2 flow at 50 $^{\circ}\text{C}$ prior to use.

*Formation of Free-standing PS-*b*-PMMA Film:* Cylinder-forming PS-*b*-PMMA ($M_n(\text{PS}) = 46100$ g/mol, $M_n(\text{PMMA}) = 21000$ g/mol; $M_w/M_n = 1.09$) and lamella-forming PS-*b*-PMMA ($M_n(\text{PS}) = 53000$ g/mol, $M_n(\text{PMMA}) = 54000$ g/mol; $M_w/M_n = 1.16$) diblock copolymers were purchased from Polymer Source. The domain spacing of cylinder-forming and lamella-forming PS-*b*-PMMA are 36 nm and 57 nm, respectively, according to scanning electron microscopy (SEM) observation. The BCPs were dissolved in toluene and spin-coated onto the pretreated graphene to form thin films. BCP films with different thickness were obtained by tuning the solution concentration (3.5–25 mg/mL). The BCP films were annealed at 250 $^{\circ}\text{C}$ under Ar for 30–40 h for phase separation. The Cu foil was dissolved by saturated $(\text{NH}_4)_2\text{S}_2\text{O}_8$ (Sigma Aldrich) solution. After carefully washed by deionized water, we can obtain the free-standing BCP films with nanopattern. The BCP films were fished out by different substrates, including Si wafer, indium tin oxide (ITO), polydimethylsiloxane (PDMS), and poly(ethylene terephthalate) (PET).

Deposition of Au Nanopattern: To get nanopattern of Au nanoparticles, the free-standing BCP film with lamellar-forming nanopattern was first fished out and transferred on Si wafer. To guarantee a full contact of BCP-graphene film with the Si wafer, a natural drying followed by vacuum drying procedure was applied to thoroughly remove the water between the film and the Si wafer. Next, Ar plasma treatment (50 W, 20 sccm Ar) was conducted on the BCP to remove PMMA blocks and the underneath graphene, thus obtaining the template of PS blocks.

Au nanoparticles were deposited in the intervals of PS blocks by galvanic displacement. For the galvanic displacement, the Si wafer coated with BCP film was immersed in 1% (v/v) HF solution for 20 s and then in a mixture solution of 1 mL 1% (v/v) HF, 3mL 10 wt% HAuCl₄ and 1 mL alcohol for 40 s, followed by washing with deionized water. Finally, we removed PS template and the residual graphene simply by peeling off them with an adhesive tape and obtained the nanopattern of Au.

Characterizations: The surface morphology of the BCP films was observed by Hitachi S-4800 SEM with a field emission source of 10 kV. To increase the SEM contrast, all the annealed samples were treated with Ar plasma to selectively remove the PMMA domains. Raman spectra of graphene were collected with a Microscope Raman Spectroscopy (Thermo Scientific DXR) motivated by 532 nm laser. The surface elemental information was analyzed by the X-ray photoelectron spectroscopy (XPS) on the Thermo Scientific ESCALab 250Xi using 200 W Al K α radiation. Contact angles (θ_w) of various solvents on the pretreated graphene were performed by optical contact angle measuring device (DSA 100, KRUSS). Each θ_w is the average value measured in different position of the sample. The film thickness of BCP was determined by spectroscopic ellipsometer (SE 850 DUV, SENTECH Instruments).

Table S1. Contact angles of different solvents on UVO treated graphenes.

solvent	Contact angle (°)	
	G-5*	G-7*
water	77.87	73.39
ethylene glycol	55.30	52.03
formamide	61.61	60.38
glycerol	62.25	59.65

* G-5 and G-7 represents the graphene films treated by UVO for 5 min and 7 min, respectively.

Neumann's method is applied to calculate their surface energies. The surface energies of G-5 and G-7 are (59.0 ± 0.4) mJ/m² and (60.1 ± 0.3) mJ/m², respectively. Wang et al¹ have determined the surface energies of graphene (46.7 mJ/m²) and graphene oxide (62.1 mJ/m²).

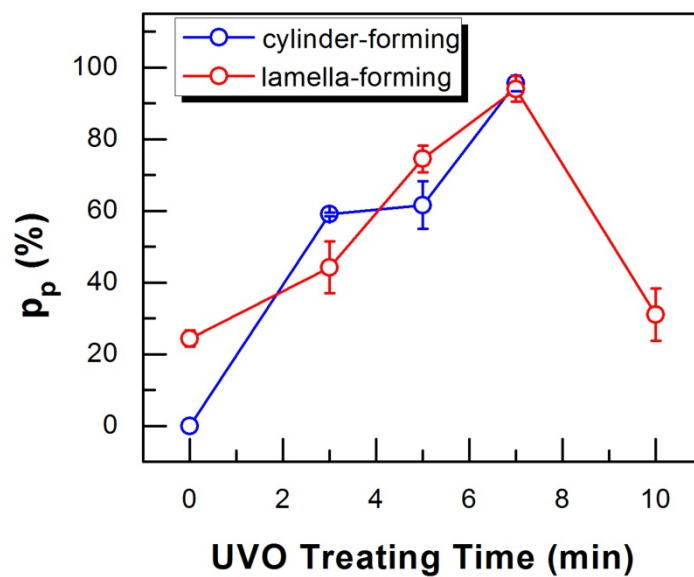


Fig. S1 Evolution of the percentage of perpendicularly oriented microdomains (p_p) in BCP film with the UVO treating time of graphenes. We conducted the statistical analysis based on 3–5 SEM images of each sample in different zones. The value of p_p is obtained by calculating the ratio of perpendicularly oriented microdomains over the whole area of the SEM image. The morphology of cylinder-forming microdomains becomes sparse array when UVO treating time is 10 min, so p_p at 10 min is meaningless in this case and is not included in the statistics.

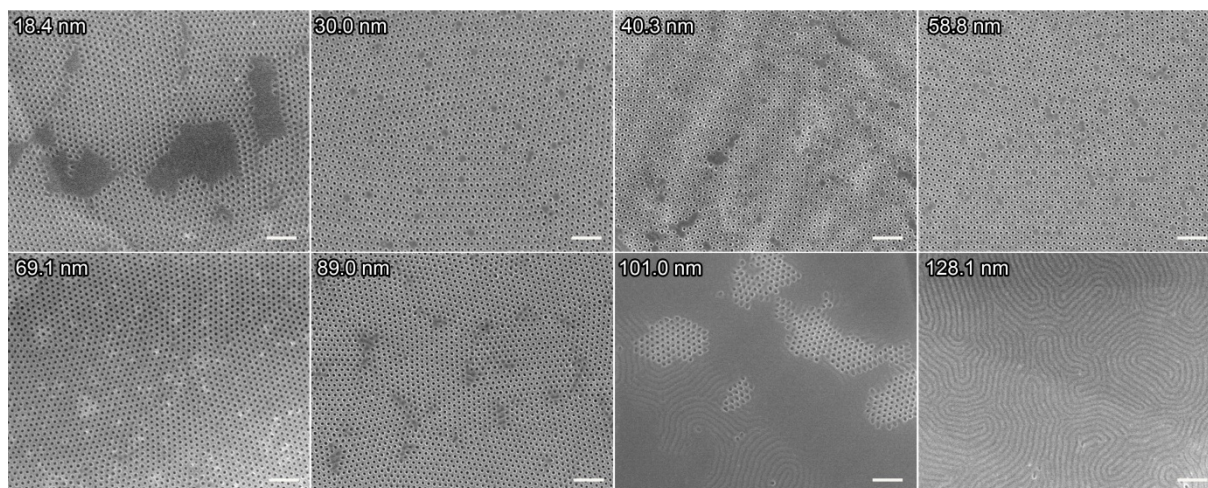


Fig. S2 SEM images of the cylinder-forming PS-*b*-PMMA of various film thicknesses on the graphene films exposed to UVO for 7 min (scale bar: 200 nm).

When the film thickness is 18 nm or less, regions without orientation feature can be observed, although a majority of the BCP film shows perpendicular orientation structure. For the films with a thickness of 30–89 nm, highly ordered cylinder microdomains are observed perpendicular to the film surface. For the film further increased to 101 nm or thicker, the parallel orientation morphology arises.

Generally, the thickness dependence of the perpendicular orientation microdomains results from the boundary conditions of substrate and free surface (atmosphere). In this case, graphene (neutral surface) and Ar (free surface, slightly prefers to PS) determine the morphology of BCP films together. For the film of suitable thickness, the effect of neutral graphene substrate is enough to form a perpendicular orientation of microdomains. For the film that is too thin, the film thickness is insufficient to cover the whole surface during the thermal annealing, leading to only partial area of perpendicular orientation. For the film thickness that is exceedingly thick, the effect of neutral substrate (graphene) decays while the boundary condition of free surface (atmosphere) dominates, so the perpendicular orientation at the free surface degrades and the parallel orientation dominates the whole nanostructure.

Similar phenomena of perpendicular feature dependence on the film thickness have been reported when using the P(S-r-MMA) as neutral surface.²⁻⁴

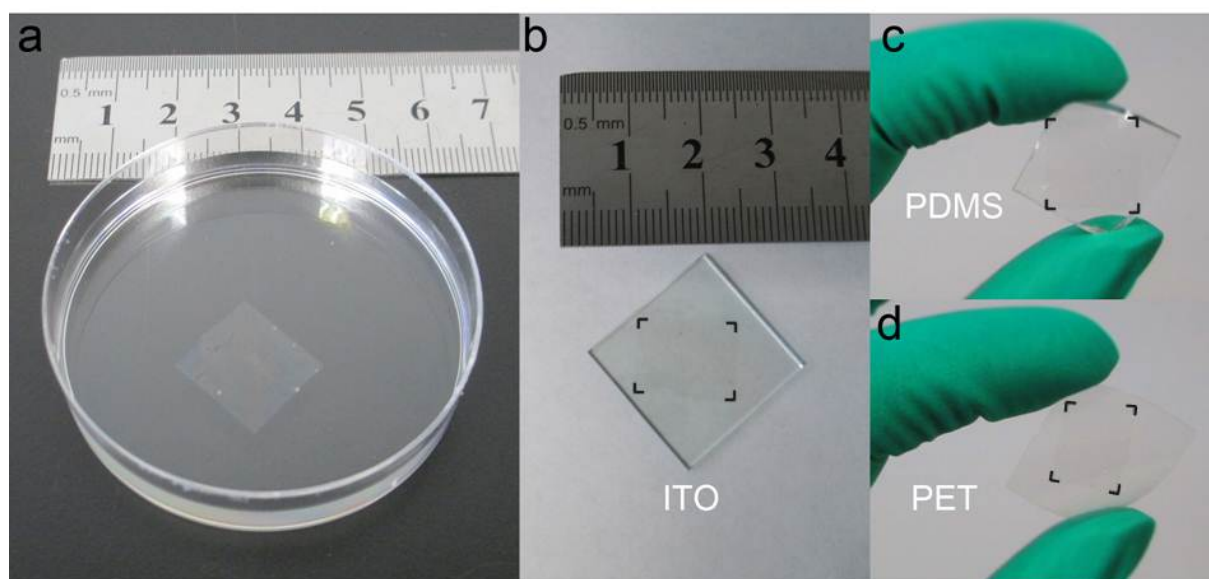


Fig. S3 Digital images of (a) free-standing PS-*b*-PMMA film floating on deionized water; and the free-standing film transferred onto (b) ITO substrate, (c) PDMS substrate and d) PET substrate.

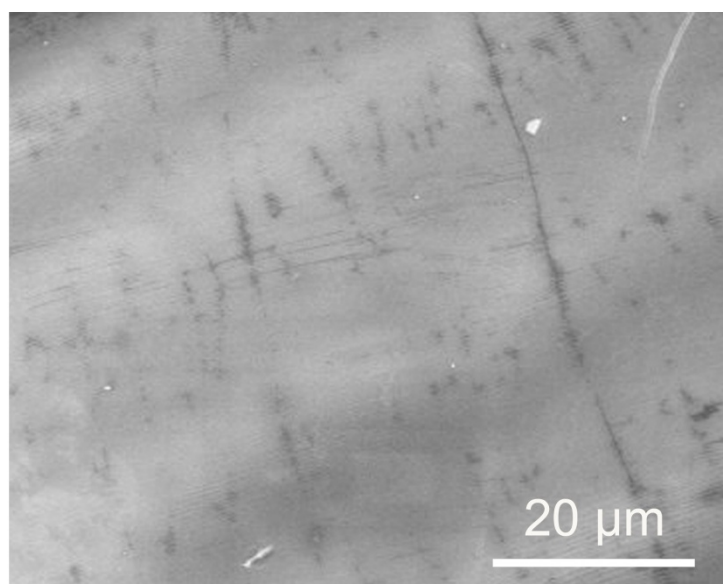


Fig. S4 SEM image of a large areal BCP film transferred on Si wafer, where the uniform contrast suggests that the large areal film have the same morphology of perpendicular microdomain orientation (high magnification image shown in Fig. 4b).

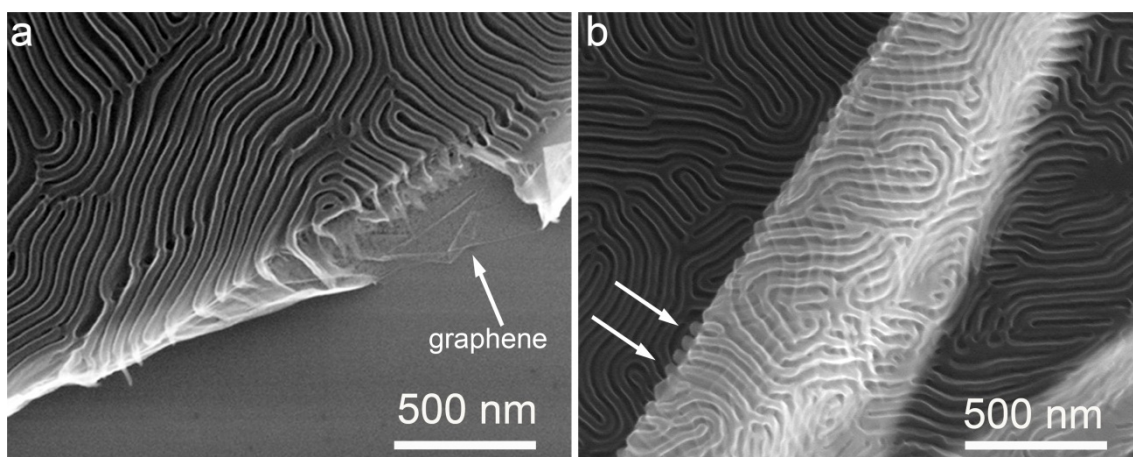


Fig. S5 (a) Side view of the edge of the BCP films. The arrow indicates the graphene beneath the BCP films. (b) A top-down view SEM image of folded BCP films on Si wafer. Even though folded and fractured indicated by the arrows, the fingerprint morphology stays intact as shown by the overlapping fingerprint area.

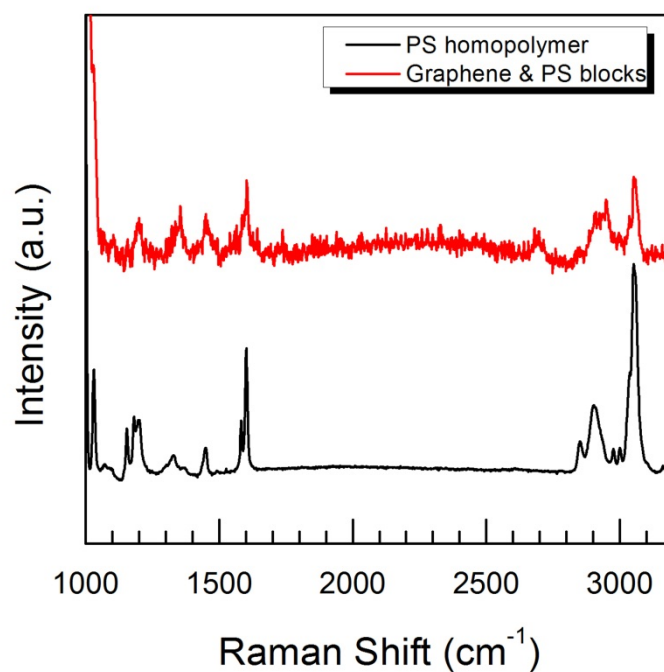


Fig. S6 Raman spectra of PS homopolymer film and PS template with graphene beneath.

References:

1. S. Wang, Y. Zhang, N. Abidi and L. Cabrales, *Langmuir*, 2009, **25**, 11078-11081.
2. H. S. Suh, H. Kang, P. F. Nealey and K. Char, *Macromolecules*, 2010, **43**, 4744-4751.
3. E. Han, K. O. Stuen, Y.-H. La, P. F. Nealey and P. Gopalan, *Macromolecules*, 2008, **41**, 9090-9097.
4. C. M. Bates, J. R. Strahan, L. J. Santos, B. K. Mueller, B. O. Bamgbade, J. A. Lee, J. M. Katzenstein, C. J. Ellison and C. G. Willson, *Langmuir*, 2011, **27**, 2000-2006.